Chemical Physics 142 (1990) 123–131
North-Holland

ABSORPTION AND EMISSION SPECTROSCOPIC INVESTIGATION OF CYANOVINYLDIETHYLANILINE DYE VAPORS

A.V. DESHPANDE [1], A. BEIDOUN, A. PENZKOFER
Naturwissenschaftliche Fakultät II–Physik, Universität Regensburg, D-8400 Regensburg, FRG

and

G. WAGENBLAST
BASF Aktiengesellschaft, D-6700 Ludwigshafen, FRG

Received 28 September 1989

The dyes 4-dicyanovinyl-N,N-diethylaniline (DCVA) and 4-tricyanovinyl-N,N-diethylaniline (TCVA) are investigated spectroscopically in the vapor phase. The absorption and emission spectra are compared with solution spectra. The thermal stability of the dye powder is determined. The saturated vapor density versus temperature is deduced from absorption measurements. The vapor absorption peaks at 382 nm (DCVA) and 437 nm (TCVA). The fluorescence quantum efficiency of both dyes in the vapor phase is approximately 1.5×10^{-4}.

1. Introduction

The aniline (styryl) dyes 4-dicyanovinyl-N,N-diethylaniline (DCVA, 4-diethylamino-β,β-dicyanostyrene [1], *p*-diethylaminobenzolmalonitrile [2]) and 4-tricyanovinyl-N,N-diethylaniline (TCVA, 4-diethylamino-α,β,β-tricyanostyrene [1]) belong to the dipolar meropolymethine group [3]. Their structural formulae are shown in figs. 4 and 5 below. They are used for coloring synthetic polymer fibers [1] and are applied as sublimable dyes in heat-transfer recording materials [4,5] and in photoconductive recording materials [6].

In this paper the usability of these dyes as gain media in dye vapor lasers is investigated. For this purpose thermodynamic and spectroscopic properties of the dyes are studied. Absorption and fluorescence spectra of the dye vapors are determined and compared with solution spectra. The fluorescence quantum efficiency is found to be very small ($q\approx1.3\times10^{-4}$ for DCVA, and $q\approx1.6\times10^{-4}$ for TCVA). The thermal stability of the dyes is tested [7] and the saturated vapor density versus temperature is deduced from absorption measurements [7–9].

[1] On leave from Department of Chemical Technology, University of Bombay, Bombay 400 019, India.

0039-6028/90/$ 03.50

2. Experimental

The thermal stability of the dye stuff is investigated by heating the dye materials in an evacuated stainless steel vessel and determining the fraction of undestroyed dye. The absorption spectra of solutions of heated and unheated dye are compared. The technique is described in ref. [7].

The spectroscopic measurements are carried out by using a stainless steel vapor cell with sapphire windows (cell length 5 cm). Details of the vapor cell are given in ref. [8]. The transmission measurements are performed in a conventional spectrophotometer (Beckman type Acta MIV) [7,8].

The absolute absorption cross sections $\sigma(\lambda)$ of the vapors are calculated by equating the total S_0–S_1 absorption cross-section integrals of the vapors and the

dye solutions in cyclohexane, i.e. it is set $\int_{abs}\sigma(\tilde{\nu})\,d\tilde{\nu}=\int_{abs}\sigma_L(\tilde{\nu})\,d\tilde{\nu}$ [7.9] ($\tilde{\nu}=\lambda^{-1}$ is the wavenumber, $\sigma_L(\tilde{\nu})$ is the absorption cross section of the solution at wavenumber $\tilde{\nu}$). The integrals extend over the S_0–S_1 absorption bands (abs). A good agreement between the S_0–S_1 absorption cross-section integrals of dye vapors and dye solutions was found in previous studies on organic dyes [8–11]. Some reasoning of the equality of the absorption cross-section integrals is given in ref. [10].

The saturated vapor densities N_S are derived from the transmission measurements by

$$N_S=-\ln[T(\lambda_{a,p})]/\sigma(\lambda_{a,p})l, \qquad (1)$$

where $\lambda_{a,p}$ is the wavelength of maximum S_0–S_1 absorption and l is the vapor cell length. Surplus dye is inserted in the dye reservoir to achieve an equilibrium between the condensed dye and the dye in the vapor phase.

The fluorescence spectra are measured with a homemade spectrofluorometer [12]. The front-face collection technique is applied. A mercury lamp (Osram HBO 200 W/4) combined with interference filters serves as excitation source. The fluorescence quantum efficiencies are obtained by comparing the fluorescence signals of the vapors with the fluorescence signals of standard solutions of known quantum efficiency.

3. Results

3.1. Thermal stability

The thermal stability of the dyes is determined by comparing absorption spectra of methanolic solutions of heated and unheated dye stuff. The ratios

$$r=\frac{\ln[T(\lambda)]V/m_{inw}l}{\ln[T_{nh}(\lambda_{a,p})]V_{nh}/m_{inw,nh}l_{nh}} \qquad (2)$$

are compared. In the denominator are the parameters of the nonheated reference sample while in the numerator are the parameters of the heated sample. m_{inw} is the mass of dye inweighted. V is the volume of the solution. l is the length of the transmission measurement cell.

Fig. 1 presents examples for DCVA. The solid curve is the normalized absorption spectrum of untreated dye (absorption peak at 435 nm). The dashed curve shows the spectral changes of a sample heated to 230°C for 1.2 h. The total absorption integral decreases, indicating the decomposition in volatile components. A product absorbing at longer wavelength is formed (peak absorption around 500 nm). Heating the dye to 230°C for 3.1 h (dash-dotted curve) causes a nearly complete destruction of the dye.

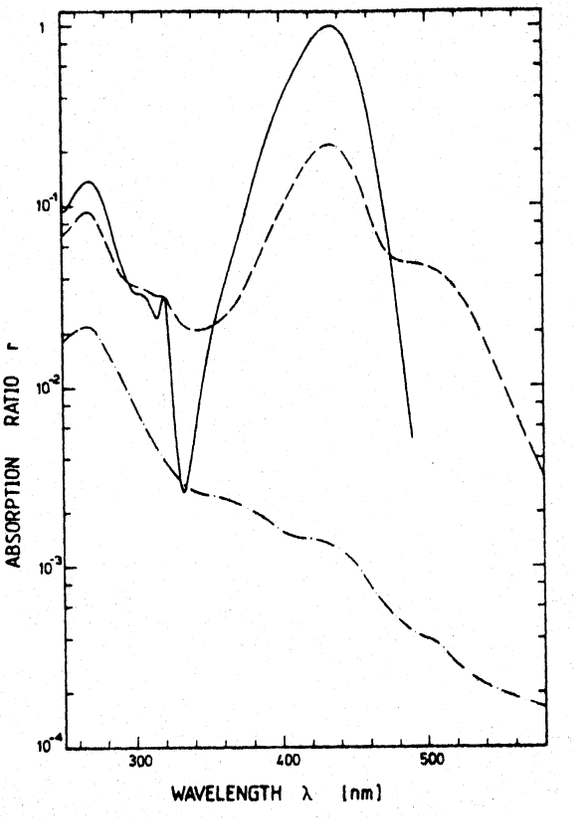

Fig. 1. Spectral analysis of thermal stability of DCVA powder. Solid curve, unheated dye. Dashed curve, temperature 230°C, heating period 1.2 h. Dash-dotted curve, temperature 230°C, heating period 3.1 h.

The thermal decomposition of TCVA is illustrated in fig. 2. The dashed curve belongs to a heating period of 2.2 h at 230°C and the dash-dotted curve is measured for a heating period of 3.1 h at 230°C. Again a component absorbing at longer wavelengths is formed (absorption peak around 600 nm). One decomposition component has its absorption peak at 435 nm. This absorption peak coincides with the ab-

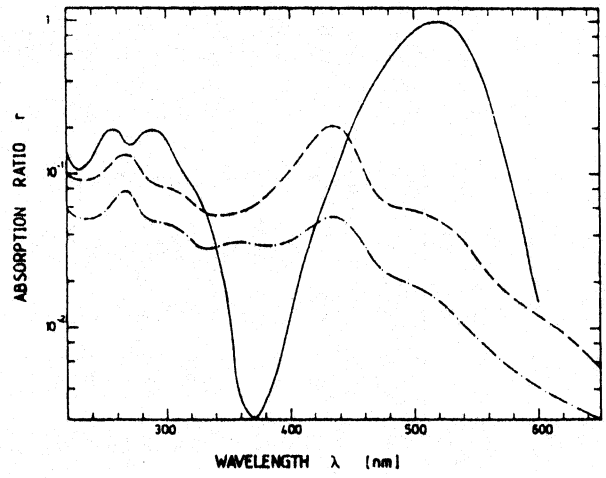

Fig. 2. Spectral analysis of thermal stability of TCVA powder. Solid curve, unheated dye. Dashed curve, 230°C for 2.2 h. Dash-dotted curve, 230°C for 3.1 h.

sorption peak of DCVA. It may be that TCVA decomposes partially into DCVA.

In the region of the S_0–S_1 absorption band of the untreated dye the absorption ratios of the heated dye components are deconvoluted roughly and the ratio of the absorption peak of undestroyed dye to the absorption peak of untreated dye determines the fraction of undestroyed dye. This fraction is plotted in fig. 3 versus heating time for different heating temperatures. Below 200°C the dyes are very stable. The experimental points indicate an over-exponential decomposition process. The disintegration products seem to enhance the decomposition rate.

3.2. Absorption spectra

The absorption spectra of DCVA vapor and TCVA vapor are shown in figs. 4 and 5, respectively. The corresponding spectra of the dye solutions in cyclohexane are included. The absolute absorption cross sections of the vapors are determined by [8–11]

$$\sigma(\tilde{\nu}) = \frac{\ln[T(\tilde{\nu})]\int_{abs}\sigma_L(\tilde{\nu})\,d\tilde{\nu}}{\int_{abs}\ln[T(\tilde{\nu})]\,d\tilde{\nu}}, \qquad (3)$$

where the S_0–S_1 absorption integrals of the vapors are set equal to those of the solutions ($\int_{abs}\sigma_L(\tilde{\nu})\,d\tilde{\nu} = \int_{447nm}^{333nm}\sigma_L(\tilde{\nu})\,d\tilde{\nu} \approx 6\times10^{-13}$ cm for DCVA in cyclohexane and $\int_{abs}\sigma_L(\tilde{\nu})\,d\tilde{\nu} = \int_{525nm}^{350nm}\sigma_L(\tilde{\nu})\,d\tilde{\nu} \approx 4.8\times10^{-13}$ cm for TCVA in cyclohexane; the integration regions of the vapors are 430–325 nm for DCVA and 490–340 nm for TCVA). The vapor spectra are blue shifted ($\Delta\tilde{\nu}_{a,p} = \tilde{\nu}^V_{a,p} - \tilde{\nu}^L_{a,p} \approx 2300$ cm^{-1} for DCVA and ≈ 2500 cm^{-1} for TCVA). The vapor spectra are smoothed compared to the cyclohexane spectra (thermal smoothing).

3.3. Saturated vapor density

The saturated vapor density, N_S, versus vapor reservoir temperature is displayed in fig. 6. The vapor cell temperature, ϑ, is kept 15°C higher than the reservoir temperature, ϑ_R, to avoid dye condensation at the sapphire windows. The values indicated by circles are obtained while heating up and those indicated by triangles are measured while cooling down. They show the same temperature dependence.

The saturated vapor densities, N_S, may be transferred to saturated vapor pressures, p_S, by application of the ideal gas equation,

$$p_S = N_S k_B \vartheta, \qquad (4)$$

where k_B is the Boltzmann constant.

The saturated vapor pressure or the saturated vapor density may be determined theoretically from the thermal equilibrium condition where the rate of desorption and the rate of adsorption at the condensed dye surface are equal [8,9]. The adsorption rate is [8,9,13–15].

$$n_{ad} = n_\downarrow S = \frac{p_S S}{(2\pi m k_B \vartheta_R)^{1/2}} = \left(\frac{k_B}{2\pi m \vartheta_R}\right)^{1/2} \vartheta N_S S, \qquad (5)$$

where m is the molecular mass and S the dye–dye sticking coefficient. The desorption rate is [8,9,15]

$$n_{des} = n_{surf}\nu_{des}\exp\left(-\frac{Q_{des}}{k_B\vartheta_R}\right), \qquad (6)$$

where n_{surf} is the surface number density of dye molecules (dimension cm^{-2}) and ν_{des} the attempt frequency of desorption from the condensed dye. The exponential factor accounts for the escape probability. Q_{des} is the dye–dye desorption energy.

The equality of adsorption and desorption rate, $n_{ad} = n_{des}$, results in

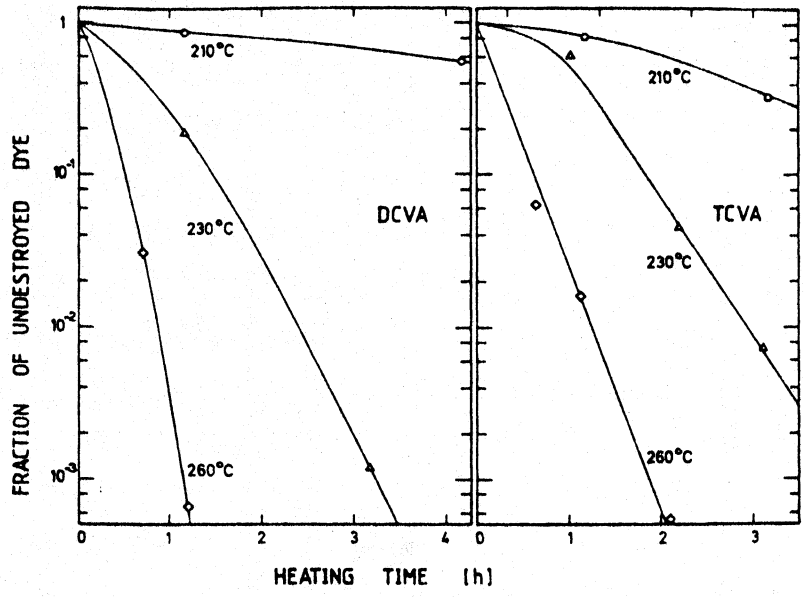

Fig. 3. Fraction of undestroyed dye versus heating time for different temperatures.

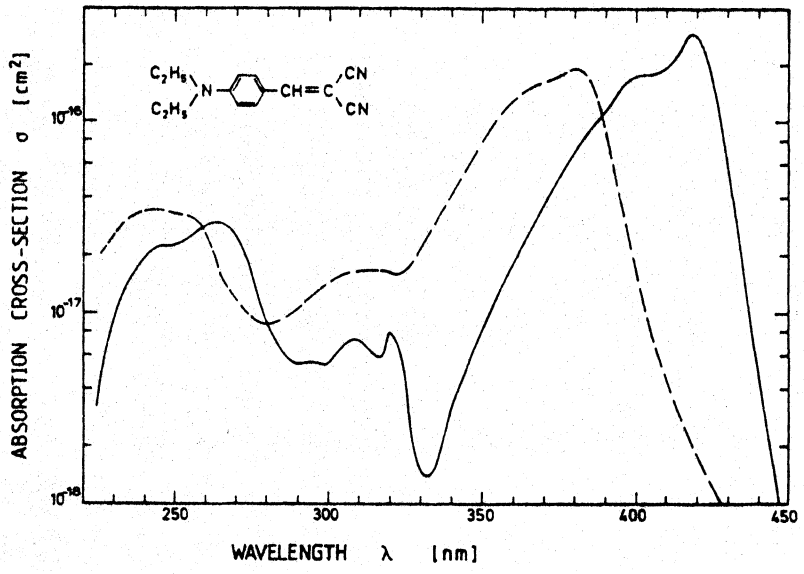

Fig. 4. Absorption cross-section spectra of DCVA in cyclohexane (solid curve) and DCVA vapor (dashed curve, $\vartheta \approx 160°C$). The structural formula of DCVA is included.

$$N_S = \left(\frac{2\pi m \vartheta_R}{k_B}\right)^{1/2} \frac{n_{surf}}{\vartheta} \frac{\nu_{des}}{S} \exp\left(-\frac{Q_{des}}{k_B \vartheta_R}\right). \quad (7)$$

Eq. (7) is fitted to the experimental points of fig. 6. For both DCVA and TCVA the surface number density is assumed to be $n_{surf} = 2 \times 10^{14}$ cm^2 (molecular size ≈ 0.5 nm^2). ν_{des}/S and Q_{des} are fitted. Two sets of parameters are needed for fitting the experi-

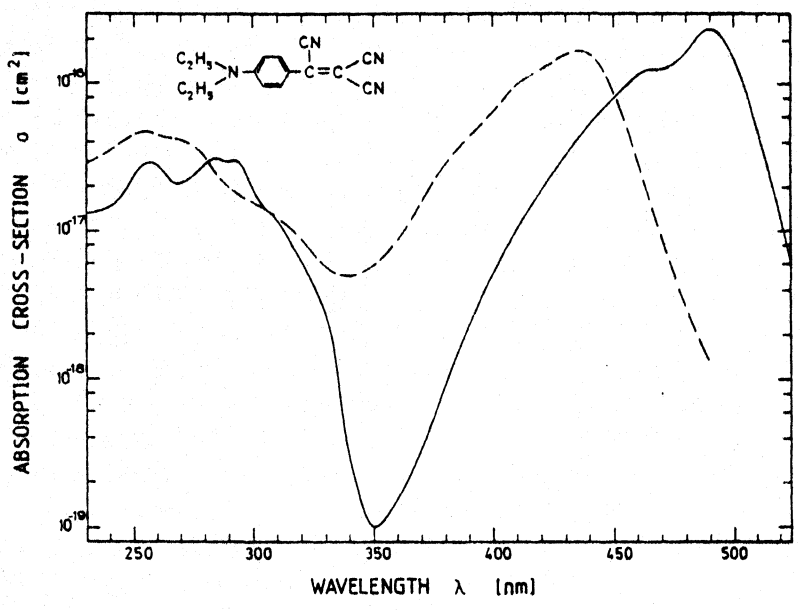

Fig. 5. Absorption cross-section spectra of TCVA in cyclohexane (solid curve) and TCVA vapor (dashed curve, $\vartheta \approx 170°C$). The structural formula of TCVA is included.

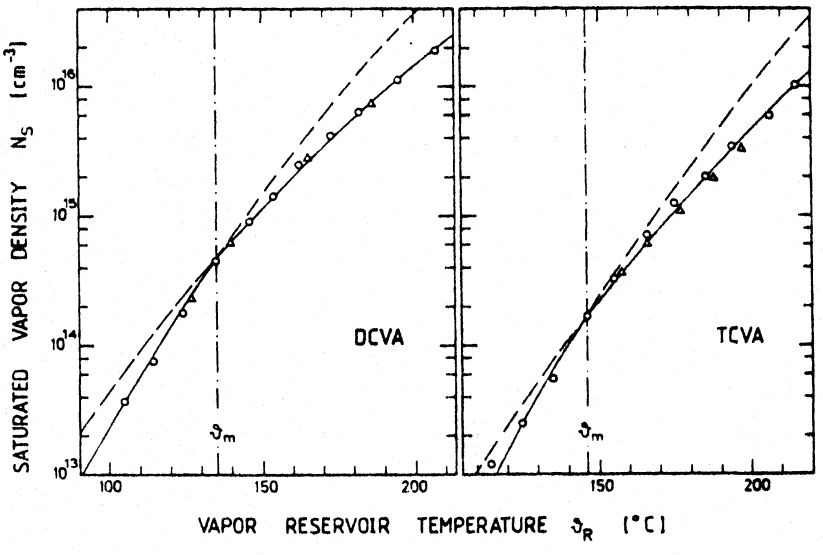

Fig. 6. Saturated vapor densities of DCVA and TCVA versus temperature. For $\vartheta_R < \vartheta_m$, sublimation. For $\vartheta_R > \vartheta_m$, evaporation. The fitted parameters of the curves are given in table 1.

mental points in the low temperature and the high temperature region. At low temperatures the dye sublimates (equilibrium between solid and vapor) while at high temperatures the dye evaporates (equilibrium between liquid and vapor). The intersection point of the curves determines the melting point, ϑ_m, of the dye. The determination of the melting temperature is not very accurate because the curves cross

Table 1
Thermodynamic properties of DCVA and TCVA

Parameter	DCVA	TCVA
sublimation		
Q_s (J)	1.82×10^{-19}	2.1×10^{-19}
ν^s_{des}/S_s (s^{-1})	1.3×10^{12}	2.2×10^{13}
evaporation		
Q_e (J)	1.44×10^{-19}	1.72×10^{-19}
ν^s_{des}/S_e (s^{-1})	1.4×10^{9}	3.1×10^{10}
melting		
Q_m (J)	3.8×10^{-20}	3.8×10^{-20}
ϑ_m (°C)	135 ±10	145 ±10

under a small angle. For DCVA a melting temperature of $\vartheta_m = 134.5 \pm 0.5$°C is reported [1]. At low temperatures Q_{des} is equal to the sublimation energy Q_s ($\Lambda_s \approx N_A Q_s$ is the molar latent heat of sublimation [9], N_A is the Avogadro constant), and at high temperatures Q_{des} is equal to the evaporation energy Q_e ($\Lambda_e \approx N_A Q_e$ is the molar latent heat of evaporation). The melting energy is $Q_m = Q_s - Q_e$ ($\Lambda_m = \Lambda_s - \Lambda_e$ is molar latent heat of melting).

The fitting parameters are listed in table 1. The surface binding energy of TCVA is slightly higher than that of DCVA (higher desorption energy, higher effective attempt frequency of escape ν_{des}/S, and higher melting temperature). The effective sublimation escape frequencies, ν^s_{des}/S_s, are considerably higher than the effective evaporation escape frequencies, ν^s_{des}/S_e. In the case of sublimation, the impinging molecules lose energy by inelastic collision. Only in the case of total loss of kinetic energy they stick to the surface. Therefore the sticking coefficient is $S_s \ll 1$. The attempt frequency of escape is the surface vibration frequency of a single molecule. In contrast, in the case of evaporation, the impinging molecules penetrate the surface and the sticking coefficient approaches toward unity ($S_e \lesssim 1$). A molecule trying to escape the liquid drags many molecules and therefore the attempt frequency of escape becomes the surface vibration frequency of many molecules which lowers ν^s_{des} compared to ν^s_{des}.

3.4. Fluorescence analysis

The fluorescence quantum distributions, $E(\lambda)$, of DCVA and TCVA vapor are determined by calibrating the spectral fluorescence distributions, $S(\lambda)$, to the total fluorescence signals, $\int_{em} S_R(\lambda)\,d\lambda$, of reference dye solutions of known quantum efficiency q_R [12,13,16] ($S(\lambda)$ and $S_R(\lambda)$ are given in photons per wavelength interval). The reference dye solutions were 9,10-diphenylanthracene in cyclohexane ($q_R = 0.90 \pm 0.02$ [17], excitation wavelength $\lambda_{exc} = 365$ nm) for DCVA vapor, and coumarin 314 T in ethanol ($q_R = 0.87 \pm 0.07$ [18], $\lambda_{exc} = 405$ nm) for TCVA vapor.

$E(\lambda)$ is given by [12,13,16]

$$E(\lambda) = \frac{S(\lambda)/W_{abs}\,\Delta\Omega}{\int_{em} S_R(\lambda)\,d\lambda / W_{abs,R}\,\Delta\Omega_R}\, q_R$$

$$= \frac{S(\lambda)}{(1-R-T)W_{exc}} \frac{(1-R_R-T_R)W_{exc,R}}{\int_{em} S_R(\lambda)\,d\lambda\, n^2_{F,R}}\, q_R \,. \tag{8}$$

The absorbed excitation energies in the dye vapor and the reference dye solution are

$$W_{abs} = W_{exc}(1-R-T)$$

and

$$W_{abs,R} = W_{exc,R}(1-R_R-T_R)\,,$$

respectively. R is the reflectivity and T is the transmission at λ_{exc}. The ratio of the solid angles of fluorescence acceptance by the detector is

$$\Delta\Omega/\Delta\Omega_R = n^2_{F,R}/n^2_F \approx n^2_{F,R}\,.$$

$n_{F,R}$ is the average refractive index of the reference solution at the wavelength of the fluorescence band. $n_F \approx 1$ is the refractive index of the dye vapor in the emission region. The spectral characteristics of the elements in the fluorescence path are taken into consideration in the determination of the fluorescence signals $S(\lambda)$ and $S_R(\lambda)$ (calibration with a halogen tungsten lamp of known colour temperature, for details see ref. [16]).

The fluorescence quantum distributions $E(\lambda)$ of DCVA and TCVA vapor are depicted in fig. 7. The fluorescence signal is very weak reaching the detection limit of our home-made spectrofluorimeter. Therefore the shapes of $E(\lambda)$ are not very accurate.

The fluorescence quantum efficiencies q of the vapors are obtained by

$$q = \int_{em} E(\lambda)\,d\lambda\,. \tag{9}$$

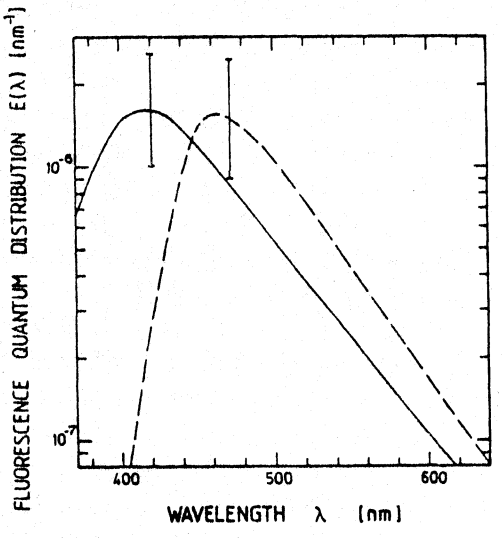

Fig. 7. Fluorescence quantum distributions of DCVA vapor (solid curve, $\vartheta \approx 150°C$) and TCVA vapor (dashed curve, $\vartheta \approx 210°C$).

The fluorescence quantum efficiencies are approximately $q \approx 1.3 \times 10^{-4}$ for DCVA vapor and $q \approx 1.6 \times 10^{-4}$ for TCVA vapor.

The radiative lifetimes, τ_{rad}, of the vapors are calculated using the Strickler–Berg formula [19,20] which exploits the fundamental relations between the transition probabilities of absorption, stimulated emission, and spontaneous emission [21]. The Strickler–Berg formula reads

$$\frac{1}{\tau_{rad}} = \frac{8\pi n_F^2 c_0}{n_A} \frac{\int_{em} E(\lambda)\,d\lambda}{\int_{em} E(\lambda)\lambda^3\,d\lambda} \int_{abs} \frac{\sigma(\lambda)}{\lambda}\,d\lambda, \qquad (10)$$

where $n_F \approx 1$ and $n_A \approx 1$ are the refractive indices of the vapors in the S_0–S_1 emission and absorption region, respectively. c_0 is the vacuum light velocity. The calculated radiative lifetimes are $\tau_{rad}(DCVA) \approx 7.2$ ns and $\tau_{rad}(TCVA) \approx 8.1$ ns. The calculated fluorescence lifetimes, $\tau_F = q\tau_{rad}$, of the vapors are $\tau_F(DCVA) \approx 0.9$ ps and $\tau_F(TCVA) \approx 1.3$ ps.

The stimulated emission cross-section spectrum is obtained from the Einstein A and B coefficients [22,23]. A short derivation is given in the appendix. The result is

$$\sigma_{em}(\lambda) = \frac{\lambda^4 E(\lambda)}{8\pi n_F^2 c_0 \tau_{rad} q}. \qquad (11)$$

In fig. 8 the absorption cross-section spectra, $\sigma(\lambda)$, and the emission cross-section spectra $\sigma_{em}(\lambda)$ of the DCVA and TCVA vapors are displayed. The σ_{em} spectra are very crude because $E(\lambda)$ is known only very inaccurately.

4. Conclusions

In this paper thermodynamic and spectroscopic parameters of the styryl dyes (aniline dyes) DCVA and TCVA have been determined. The dyes are thermally stable up to 200°C. The saturated vapor densities at 200°C are rather high corresponding to vapor densities of $N_S(DCVA) \approx 1.4 \times 10^{16}$ cm^{-3} and $N_S(TCVA) \approx 4.5 \times 10^{15}$ cm^{-3}. The fluorescence quantum efficiency is very low ($q(DCVA) \approx 1.3 \times 10^{-4}$, $q(TCVA) \approx 1.6 \times 10^{-4}$). This fact hinders the application of the dyes as gain media in dye vapor lasers. If the excited-state absorption of the dye vapors is weak for excitation wavelengths in the S_0–S_1 absorption region, the dye vapors may be applied as fast saturable absorbers [24] for dye lasers in the blue and violet spectral region ($350 \lesssim \lambda \lesssim 390$ nm for DCVA vapor, and $400 \lesssim \lambda \lesssim 450$ nm for TCVA vapor). Ultrashort pulse generation by amplified spon-

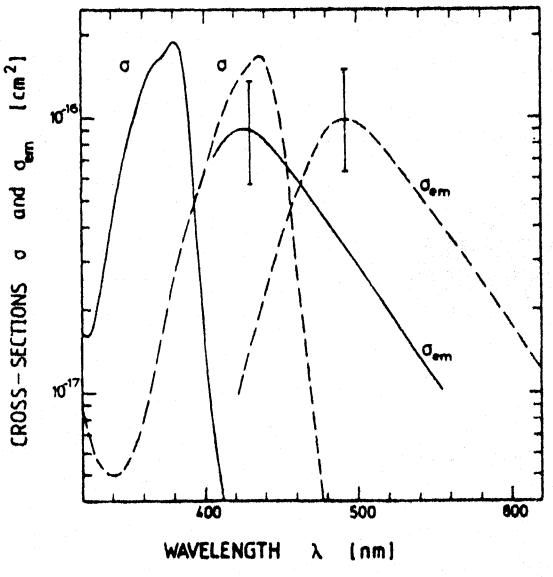

Fig. 8. Absorption cross section, σ, and emission cross section, σ_{em}, spectra of DCVA vapor (solid) and TCVA vapor (dashed).

taneous emission [25,26] may be possible by femtosecond pulse excitation [27].

Acknowledgement

The authors thank Dr. J. Schmidt for discussions and experimental help. They thank the Deutsche Forschungsgemeinschaft for financial support.

Appendix. Relation between stimulated emission cross-section spectrum and radiative lifetime

The rate of spontaneous emission τ_{rad}^{-1} is given by the Einstein A coefficient and is related to the Einstein B coefficient by [21,22,28]

$$\tau_{rad}^{-1} = A = \frac{8\pi h\nu^3}{c^3} B = \frac{8\pi h\nu^3 n_F^3}{c_0^3} B . \qquad (A.1)$$

$c = c_0/n_F$ is the light velocity (c_0 is the vacuum light velocity, n_F is the average refractive index in the emission region). The rate of stimulated emission in a medium with spectral photon density $n_{ph}(\nu)$ (cm^{-3} s^{-1}) and excited-state level population number density N (cm^{-3}) is

$$\frac{dn_{ph}(\nu)}{dt} = Bu(\nu)NE'(\nu) . \qquad (A.2)$$

$u(\nu) = n_{ph}(\nu)h\nu$ (J cm^{-3} s^{-1}) is the spectral energy density of the radiation field. $E'(\nu)$ is the normalized spectral fluorescence quantum distribution function, i.e. $E'(\nu) = E(\nu)/q$ and $\int_{em} E'(\nu)\, d\nu = 1$. $q = \int_{em} E(\nu)\, d\nu$ is the fluorescence quantum efficiency. Introducing the spectral light intensity $I(\nu) = u(\nu)c = u(\nu)c_0/n_F = n_{ph}(\nu)h\nu c_0/n_F$, eq. (A.2) changes to

$$\frac{dI(\nu)}{dt} = \frac{h\nu c_0}{n_F q} Bu(\nu)NE(\nu)$$

$$= \frac{h\nu}{q} BI(\nu)NE(\nu) . \qquad (A.3)$$

The spatial change of the spectral intensity $I(\nu)$ (W cm^{-2} s^{-1}) is

$$\frac{dI(\nu)}{dz} = \frac{n_F}{c_0}\frac{dI(\nu)}{dt} = \frac{h\nu n_F}{c_0 q} BE(\nu)I(\nu)N$$

$$= \sigma_{em}(\nu)I(\nu)N . \qquad (A.4)$$

Eq. (A.4) defines the stimulated emission cross section to

$$\sigma_{em}(\nu) = \frac{h\nu n_F}{c_0 q} BE(\nu)$$

$$= \frac{c_0^2}{8\pi\nu^2 n_F^2 q\tau_{rad}} E(\nu) . \qquad (A.5)$$

The last equality is obtained by insertion of eq. (A.1) into eq. (A.5). In terms of the vacuum wavelength, $\lambda = c_0/\nu$, eq. (A.5) reads

$$\sigma_{em}(\lambda) = \sigma_{em}(\nu) = \frac{\lambda^4}{8\pi n_F^2 c_0 q\tau_{rad}} E(\lambda) , \qquad (A.6)$$

where the relation $E(\nu) = E(\lambda)\, d\lambda/d\nu = E(\lambda)\lambda^2/c_0$ has been used.

References

[1] A.T. Peters and M.S. Wild, J. Soc. Dyers Colour. 93 (1977) 126, 133.
[2] S.S. Hassan, J.M. Abdella and N.E. Nashed, Mikrochim. Acta 2 (1984) 27.
[3] S. Dähne and F. Moldenhauer, J. Mol. Structure 27 (1975) 67.
[4] N. Taguchi, A. Imai, T. Niwa and Y. Murata, Eur. Pat. Appl. EP 163 145 A2 (1985).
[5] Mitsubishi Chemical Industries Co. Ltd., Japan. Kokai Tokkyo Koho JP 59/78895 A2 [84/78895] (1984).
[6] H.E. Wright and M.A. Berwick, Res. Discl. 158 (1977) 62.
[7] H. Weininger, J. Schmidt and A. Penzkofer, Chem. Phys. 130 (1989) 379.
[8] J. Schmidt and A. Penzkofer, Chem. Phys. 117 (1987) 265.
[9] J. Schmidt and A. Penzkofer, J. Chem. Phys. 91 (1989) 1403.
[10] L.E. Jacobs and J.R. Platt, J. Chem. Phys. 16 (1948) 1137.
[11] W.R. Ware and P.T. Cunningham, J. Chem. Phys. 43 (1965) 3826.
[12] A. Penzkofer and W. Leupacher, J. Luminescence 37 (1987) 61.
[13] J. Schmidt and A. Penzkofer, Chem. Phys. 133 (1989) 297.
[14] P.W. Atkins, Physical Chemistry, 2nd Ed. (Oxford Univ. Press, Oxford, 1982).
[15] L. Eckertova, Physics of Thin Films, 2nd Ed. (Oxford Univ. Press, Oxford, 1986) p. 99.
[16] W. Bäumler and A. Penzkofer, Chem. Phys. 140 (1990) 75.
[17] O.F. Eaton, EPA Newsletter 28 (1986) 21.

[18] Kodak technical data sheet.
[19] S.J. Strickler and R.A. Berg, J. Chem. Phys. 37 (1962) 814.
[20] J.B. Birks and D.J. Dyson, Proc. Roy. Soc. A 275 (1963) 135.
[21] A. Einstein, Physik. Z. 18 (1917) 121.
[22] W. Koechner, Springer Series in Optical Sciences, Vol. 1. Solid-State Laser Engineering, 2nd Ed. (Springer, Berlin, 1988) ch. 1.
[23] O.G. Peterson, J.P. Webb, W.C. McColgin and J.H. Eberly, J. Appl. Phys. 42 (1971) 1917.
[24] A. Penzkofer, Appl. Phys. B 46 (1988) 43.
[25] P. Sperber, W. Spangler, B. Meier and A. Penzkofer, Opt. Quant. Electron. 20 (1988) 395.
[26] P. Qiu and A. Penzkofer, Appl. Phys. B 48 (1989) 115.
[27] J. Hebling and J. Kuhl, Opt. Letters 14 (1989) 278.
[28] P.W. Milonni and J.H. Eberly, Lasers (Wiley, New York, 1988) ch. 7.